

## Supporting Information

### **Advanced hybrid Li-air batteries with high-performance mesoporous nanocatalysts**

Longjun Li,<sup>a</sup> Song-Hai Chai,<sup>b</sup> Sheng Dai<sup>b</sup> and Arumugam Manthiram\*<sup>a</sup>

<sup>a</sup> Materials Science and Engineering Program, Texas Materials Institute, The University of Texas at Austin, Austin, Texas 78712, USA. Email: manth@austin.utexas.edu; Fax: +1-512-471-7681; Tel: +1-512-471-1791

<sup>b</sup> Chemical Sciences Division, Oak Ridge National Laboratory, Oak Ridge, Tennessee 37831, USA.

## Experimental Section

IrO<sub>2</sub> nanopowder was synthesized by a modified Adams method as detailed in our previous report.<sup>[27]</sup> NiCo<sub>2</sub>O<sub>4</sub> nanoflakes grown onto nickel foam was obtained by a hydrothermal method followed by post-calcination in air.<sup>[29]</sup> The hydrothermal treatment was carried out once on each side to ensure the uniform distribution of catalyst on both sides. In one treatment, 0.5 mmol of Ni(NO<sub>3</sub>)<sub>2</sub>•6H<sub>2</sub>O, 1 mmol of Co(NO<sub>3</sub>)<sub>2</sub>•6H<sub>2</sub>O, and 3 mmol hexamethylene-tetramine were dissolved in a mixture of de-ionized water and ethanol (30 mL, 2:1 v/v), resulting in a mole ratio of 1 : 2 : 6. The obtained solution was transferred into a Teflon lined stainless-steel autoclave. A pre-cleaned nickel foam (2 cm × 4 cm) was immersed into the obtained solution with one side facing down. The autoclave was sealed and maintained at 90 °C for 10 h. After the solution was cooled down, the nickel foam was covered with a layer of greenish Ni-Co precursor preferably on the side facing down. The nickel foam was cleaned and subjected to the second hydrothermal treatment with the other side facing down. The nickel foam deposited with the Ni-Co precursor was finally annealed at 320 °C for 2 h in air. Greenish Ni-Co precursor precipitate in the solution was also collected, washed, and annealed with the same procedure to obtain NiCo<sub>2</sub>O<sub>4</sub> nanoflakes powder. The nickel foam with 1 mg cm<sup>-2</sup> of the NiCo<sub>2</sub>O<sub>4</sub> nanoflakes was cut into small pieces with a dimension of 0.76 cm × 0.76 cm. To obtain 0.5 mg cm<sup>-2</sup> or 2.8 mg cm<sup>-2</sup> of the NiCo<sub>2</sub>O<sub>4</sub> nanoflakes, the concentration of the solutions were adjusted while keeping the ratio of Ni(NO<sub>3</sub>)<sub>2</sub>•6H<sub>2</sub>O, Co(NO<sub>3</sub>)<sub>2</sub>•6H<sub>2</sub>O, and hexamethylene-tetramine constant.

The nitrogen-doped mesoporous carbon (N-MC) was synthesized by a direct activation of amorphous mesoporous carbon (AMC, 1.5 g) under flowing ammonia (60 mL min<sup>-1</sup>) at 1000 °C for 1 h with a heating rate of 50 °C min<sup>-1</sup>.<sup>[31]</sup> The AMC was synthesized by carbonization of nanostructured polymeric composites, which were obtained by self-assembly of block copolymer

(Pluronic F127) and phenolic resin (phloroglucinol–formaldehyde) under acidic conditions via a soft-template method.<sup>[30]</sup> In a typical synthesis, a 2 L flask was charged with 26.2 g of phloroglucinol, 52.4 g of F127, and 10.0 g of aqueous HCl (37 wt%) in 1300 mL of ethanol. The mixture was heated to reflux with stirring. To this solution, 26.0 g of aqueous formaldehyde solution (37 wt. %) was added. Precipitates appeared at about 4 min after the addition of formaldehyde, indicating the formation of F127–phenolic resin polymeric composites. The reaction mixture was stirred for 2 h and then filtered. The yellow polymer particles were washed with ethanol and dried in an oven at 100 °C for 3 h. Carbonization was carried out under flowing nitrogen (100 mL min<sup>-1</sup>) by heating the polymer particles to 900 °C with a heating rate of 2 °C min<sup>-1</sup> and maintaining the final temperature for 2 h.

The morphology and microstructure of the prepared samples were examined with a FEI Quanta 650 scanning electron microscope (SEM) and JEOL 2010F transmission electron microscope (TEM) at 200 KeV. The elemental mapping results were examined with an energy dispersive spectrometer (EDS) attached to the FEI Quanta 650 SEM. X-ray photoelectron spectroscopy (XPS) analysis was conducted with a Kratos Analytical spectrometer. The deconvolution of the XPS spectrum was performed using CasaXPS software with Gaussian-Lorentzian functions and a Shirley background. N<sub>2</sub> physisorption was performed on a Micromeritics Tristar analyzer at 77 K. Prior to the measurement, the sample was purged with flowing N<sub>2</sub> at 423 K for 2 h. The specific surface area was calculated by the Brunauer–Emmett–Teller (BET) method from the nitrogen adsorption data in the relative pressure range (P/P<sub>0</sub>) of 0.06–0.20. The total pore volume was determined from the amount of N<sub>2</sub> uptake at a relative pressure of P/P<sub>0</sub> = 0.95. The pore size distribution plot was derived from the adsorption branch of the isotherm based on the Barrett–Joyner–Halenda (BJH) model.

The linear sweep voltammetry (LSV) of N-MC and Pt/C was tested in a standard rotating disk electrode (RDE) setup with an Autolab PGSTAT302N potentiostat (Eco Chemie B.V.). The catalyst ink ( $5 \text{ mg mL}^{-1}$ ) was made by sonicating the catalyst powder (10 mg) in ethanol (2 mL). The catalyst ink (3, 5, or 7  $\mu\text{L}$ ) was then loaded onto the glassy carbon electrode (5 mm diameter) followed by drying in air. 5  $\mu\text{L}$  of Nafion solution (0.5 wt. %) was then dropped onto the top of the catalyst layer to form a protective layer. LSVs were obtained by sweeping the potential from 0.0 to -1.0 V (vs. SCE) at 1600 rpm with a scan rate of  $10 \text{ mV s}^{-1}$  in  $\text{O}_2$  saturated 0.1 M KOH solution. Chronoamperometry curves were obtained at -0.28 V and 1000 rpm. The half-cell test was conducted in a three-electrode half-cell with 0.5 M LiOH + 1 M LiNO<sub>3</sub> as the electrolyte.<sup>[27]</sup> Polarization curves were recorded on a VoltaLab PGZ 402 potentiostat by sweeping the potential at a scan rate of  $10 \text{ mV s}^{-1}$ . Chronopotentiometry data were collected on an Arbin BT 2000 battery cycler. The half-cell polarization curves and chronopotentiometry data were manually corrected for iR loss.

A PTFE layered battery mould was used to carry out the full cell test. The anode side was assembled in an argon filled glove box and then combined with the cathode side in air. The anode side consisted of a nickel foam current collector, a lithium metal foil, and the organic carbonate electrolyte (1 M LiPF<sub>6</sub> in ethylene carbonate (EC) / diethylcarbonate (DEC) (1:1 v/v)) absorbed by two layers of Celgard® polypropylene. The cathode side consisted of 2 mL of 0.5 M LiOH + 1 M LiNO<sub>3</sub> solution as the catholyte, an air electrode ( $0.76 \text{ cm} \times 0.76 \text{ cm}$ ), and a platinum mesh current collector. The method to prepare the air electrode has been reported elsewhere.<sup>[27]</sup> A LTAP ( $\text{Li}_{1+x+y}\text{Ti}_{2-x}\text{Al}_x\text{P}_3\text{-ySi}_y\text{O}_{12}$ ) membrane (0.15 mm thick,  $= 1 \times 10^{-4} \text{ S cm}^{-1}$ ,  $0.76 \text{ cm} \times 0.76 \text{ cm}$ , OHARA Inc., Japan) was used as the separator. The cell structure can be found in our previous report.<sup>S1</sup> A piece of aluminum laminate film ( $\sim 153 \mu\text{m}$  thick, Dai Nippon

Printing Co., Ltd) with a square hole ( $0.76 \text{ cm} \times 0.76 \text{ cm}$ ) in the middle acted as the sealing film for the LTAP membrane. The LTAP could be anchored on the hole of the sealing film by heating and pressing them at  $\sim 170 \text{ }^\circ\text{C}$  on a hot plate with a spatula. In the conventional air electrode, the catalysts include Pt/C (20 wt. %,  $1 \text{ mg cm}^{-2}$ , Johnson Matthey) and  $\text{IrO}_2$  nanopowder ( $1 \text{ mg cm}^{-2}$ ). In our cell with mesoporous nanocatalysts, an additional oxygen evolution electrode ( $\text{NiCo}_2\text{O}_4$  nanoflakes on nickel foam,  $1 \text{ mg cm}^{-2}$ ,  $0.76 \text{ cm} \times 0.76 \text{ cm}$ ) was immersed into the catholyte between the solid electrolyte and ORR air electrode (nitrogen-doped mesoporous carbon,  $1 \text{ mg cm}^{-2}$ ). A nickel wire was attached to the nickel foam to conduct current. The cathode side of the hybrid cell was purged with water-saturated air during operation to suppress the evaporation of water from the catholyte. The polarization curves were obtained by sweeping the potential at a scan rate of  $10 \text{ mV s}^{-1}$  with a VoltaLab PGZ 402 potentiostat. Discharge-charge experiments were conducted with an Arbin BT 2000 battery cycler with a 5-minute rest time between each discharge and charge period. For the cell with mesoporous nanocatalysts, two independent Arbin channels were used to collect the discharge and charge data alternatively with a 5-minute rest time between each discharge and charge period.

**Table S1.** Summary of the cycling performances of prominent hybrid Li-air batteries developed world-wide

No.	Catalyst	Current density	Total cycling time (h)	Round-trip overpotential increased (V)	Ref.
1	$\text{Sr}_{0.95}\text{Ce}_{0.05}\text{CoO}_{3-\delta}\text{-Cu}$	$0.2 \text{ mA cm}^{-2}$	37.5*	$\sim 0.26^*$	S2
2	Pt	$0.5 \text{ mA cm}^{-2}$	60*	$\sim 0.26^*$	S3
3	N-doped carbon nanotubes grown onto carbon fiber paper	$0.5 \text{ mA cm}^{-2}$	65	0.23	20
4	Heat-treated graphene nanosheets	$0.5 \text{ mA cm}^{-2}$	200	$\sim 0.23^*$	18
5	Stainless steel + commercial ORR electrode (decoupled)	$2 \text{ mA cm}^{-2}$	<200 (Li-water)	$\sim 0.16^*$	12
6	Titanium + $\text{Mn}_3\text{O}_4/\text{C}$ (decoupled)	$0.5 \text{ mA cm}^{-2}$	80	$\sim 0.21^*$	13
7	NCONF@Ni + N-MC (decoupled)	$0.5 \text{ mA cm}^{-2}$	400	0.08	This work

\* Data were obtained by analyzing the published data and figures.

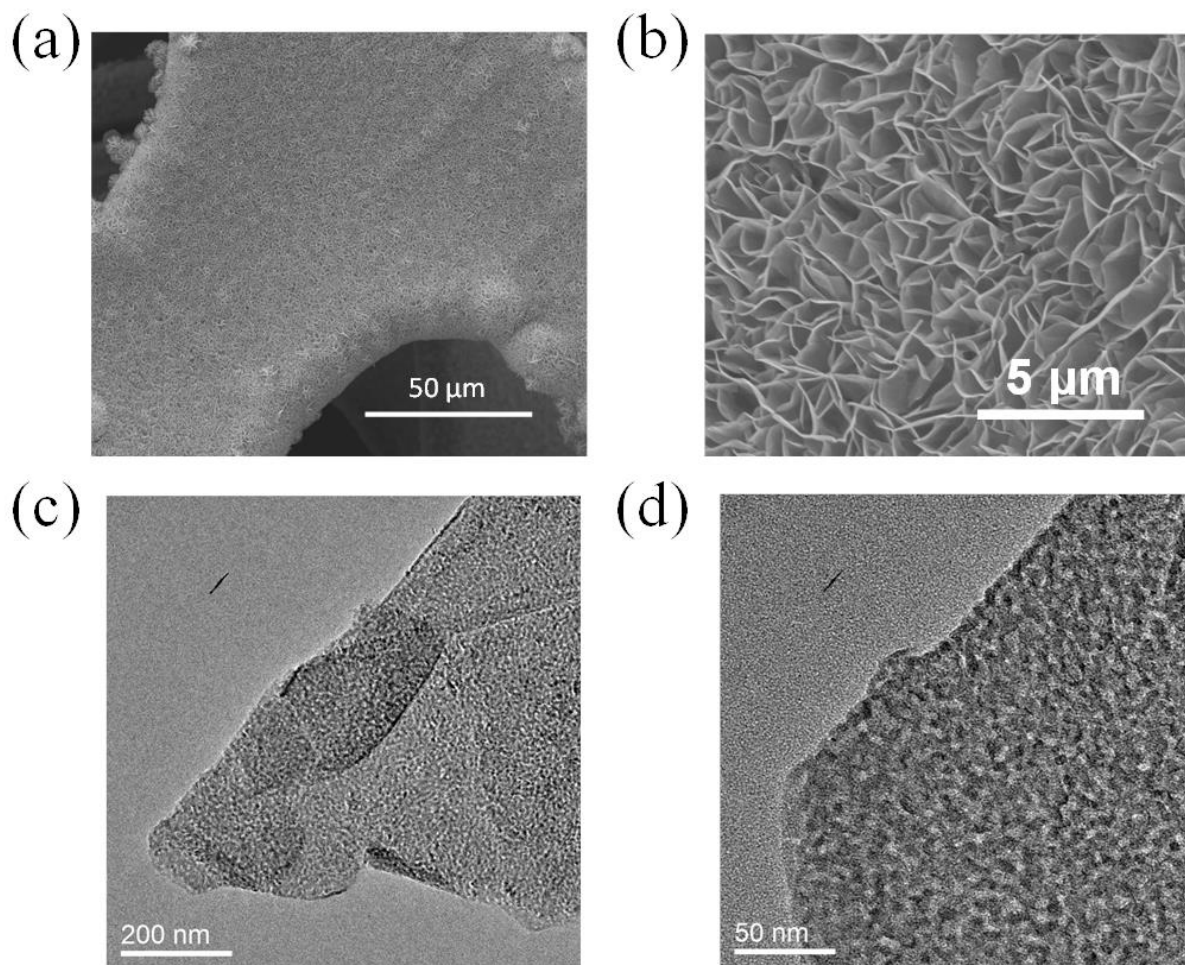


**Figure S1.** SEM and TEM images of the synthesized  $\text{NiCo}_2\text{O}_4$  nanoflakes on the nickel foam.

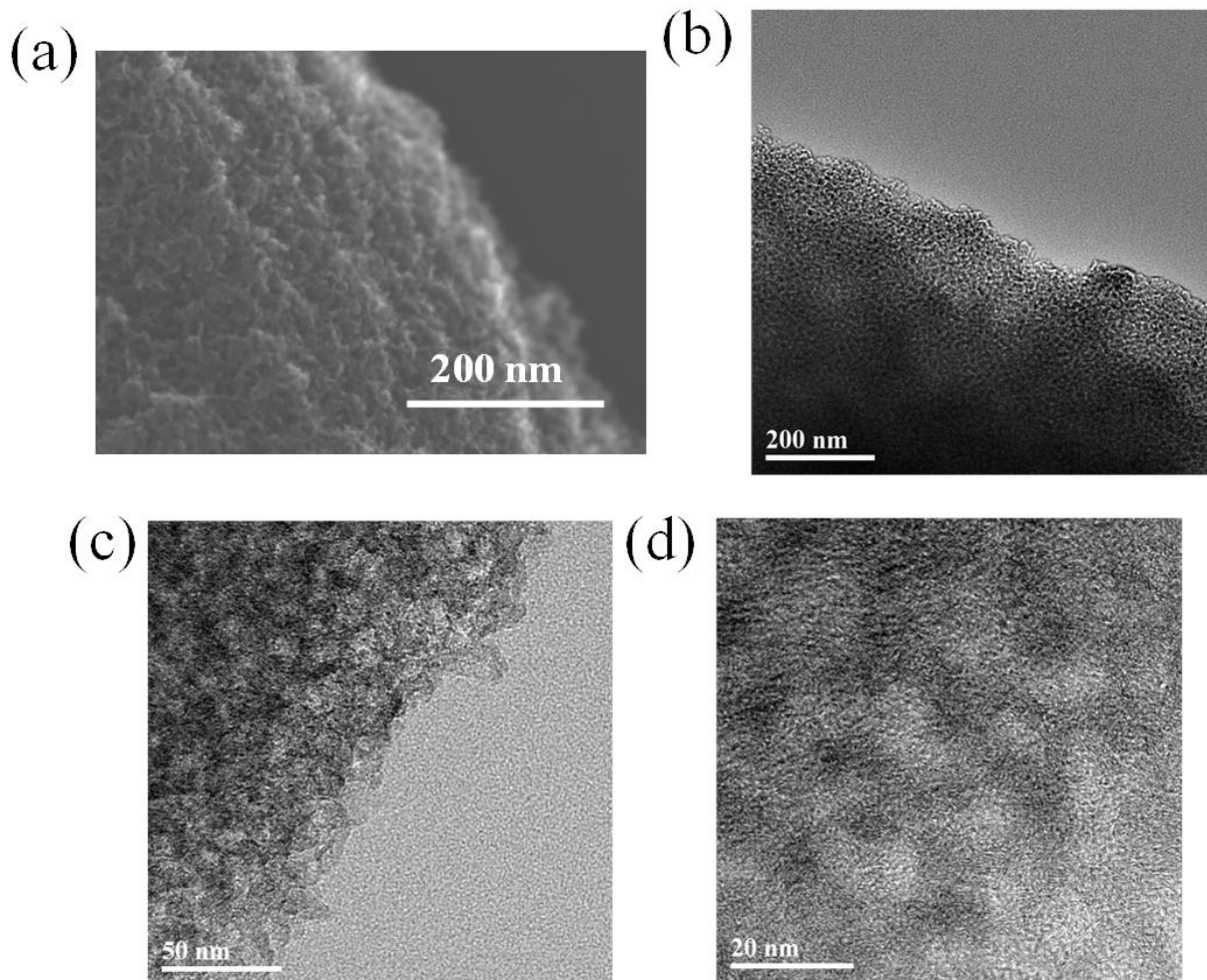


**Figure S2.** SEM and TEM images of the synthesized N-doped mesoporous carbon.



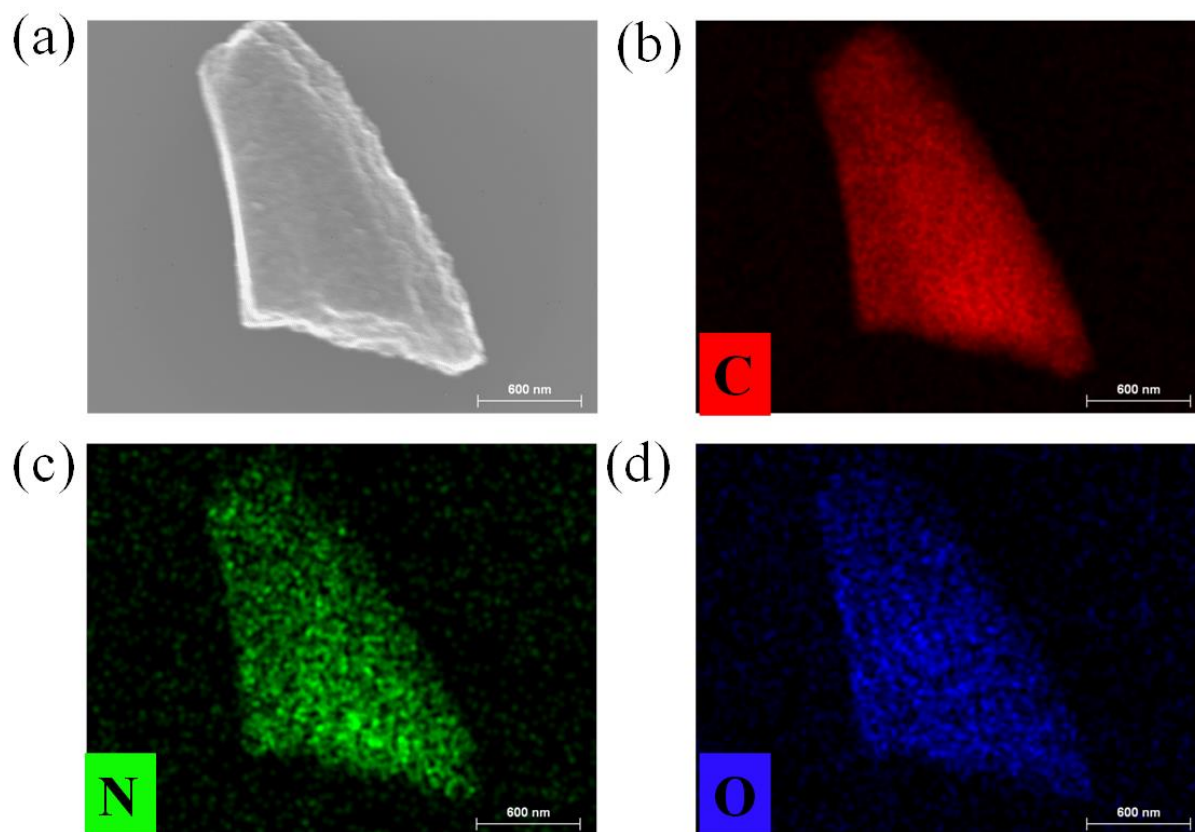


**Figure S3.** SEM image and EDX mappings of one single N-doped mesoporous carbon particle.

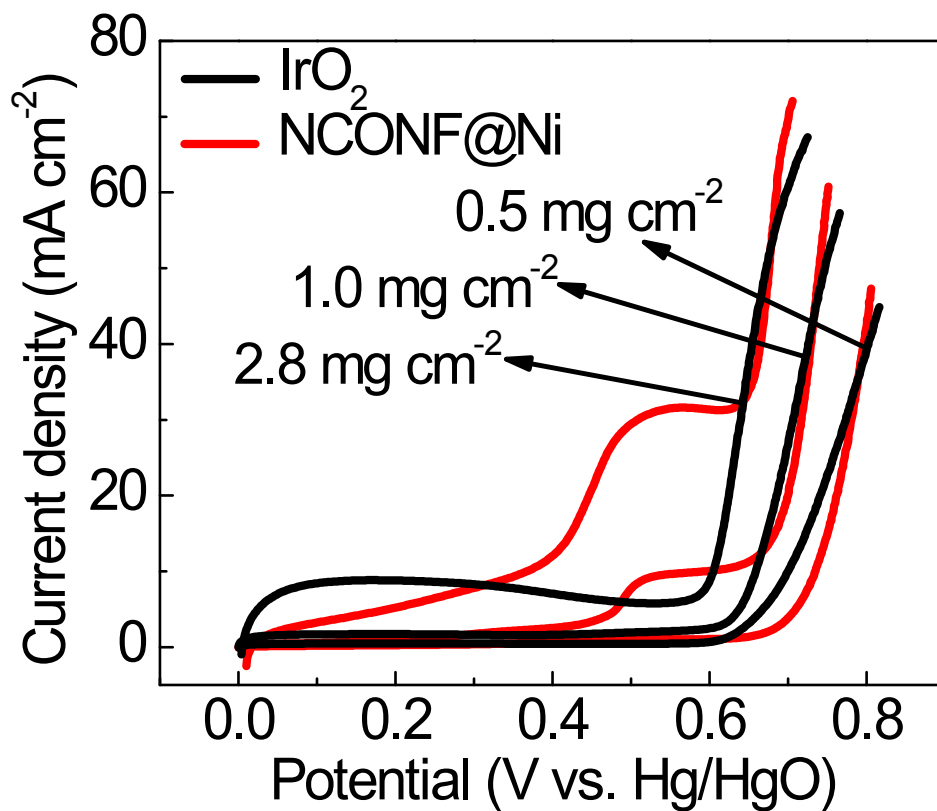


**Figure S4.** Loading-dependent polarization curves of IrO<sub>2</sub> and NCONF@Ni.

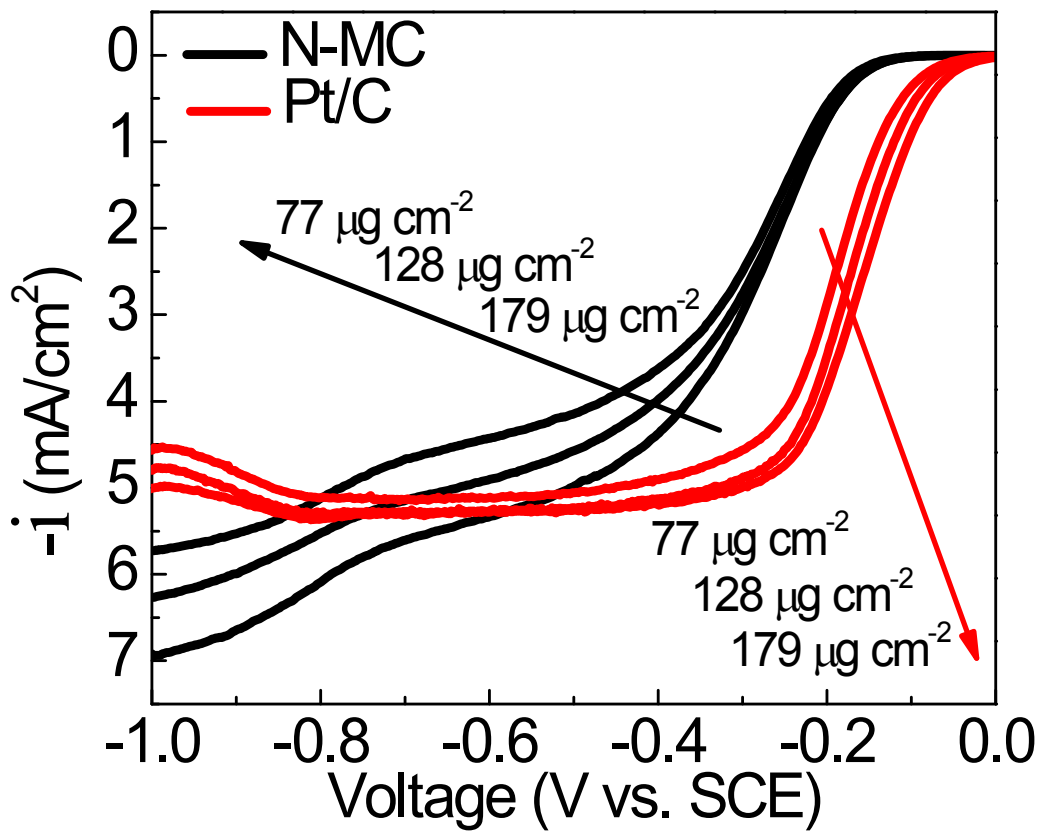


**Figure S5.** Loading-dependent polarization curves of N-MC and Pt/C.

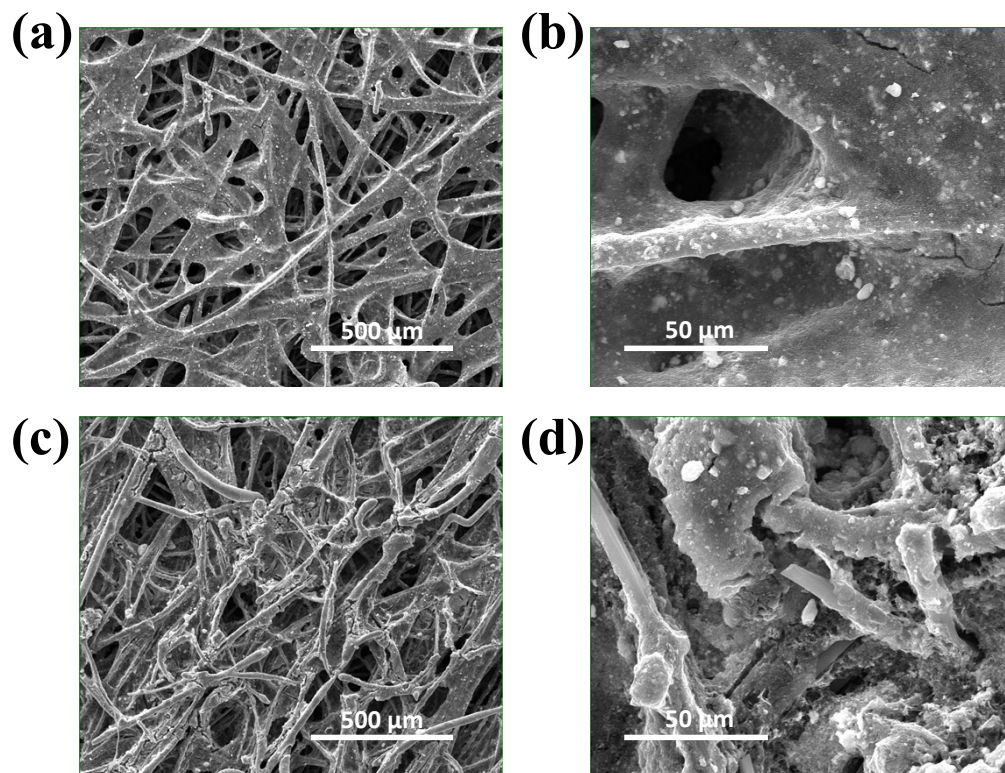
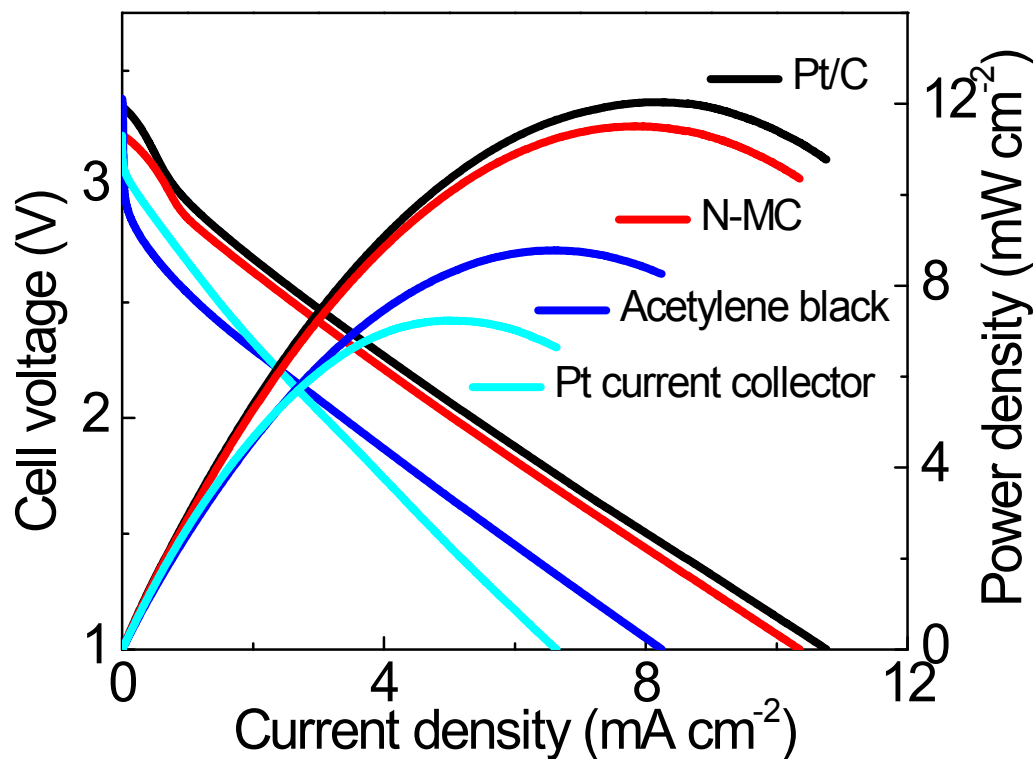


Figure S6. SEM images of Pt/C + IrO<sub>2</sub> air electrode (a,b) before and (c,d) after the cycling test.



**Figure S7.** ORR polarization curves of N-MC, Pt/C, carbon black, and Pt current collector in hybrid Li-air cells. All catalysts were tested with Pt mesh current collector.

## References

- S1. L. Li, X. Zhao and A. Manthiram, *Electrochem. Commun.*, 2012, **14**, 78-81.
- S2. W. Yang, J. Salim, S. Li, C. Sun, L. Chen, J. B. Goodenough and Y. Kim, *J. Mater. Chem.*, 2012, **22**, 18902-18907.
- S3. T. Zhang, N. Imanishi, Y. Shimonishi, A. Hirano, Y. Takeda, O. Yamamoto and N. Sammes, *Chem. Commun.*, 2010, **46**, 1661-1663.

